Research
Clean Energy—Article

A Comprehensive Approach for the Clustering of Similar-Performance Cells for the Design of a Lithium-Ion Battery Module for Electric Vehicles

Wei Li [a], Siqi Chen [b], Xiongbin Peng [b], Mi Xiao [a], Liang Gao [a,*], Akhil Garg [b], Nengsheng Bao [b]

[a] State Key Lab of Digital Manufacturing Equipment and Technology, Huazhong University of Science and Technology, Wuhan 430074, China
[b] Key Lab of Mechatronic Systems Intelligent Integration Technology, Ministry of Education, Shantou University, Shantou 515063, China

ARTICLE INFO

ABSTRACT

An energy-storage system comprised of lithium-ion battery modules is considered to be a core component of new energy vehicles, as it provides the main power source for the transmission system. However, manufacturing defects in battery modules lead to variations in performance among the cells used in series or parallel configuration. This variation results in incomplete charge and discharge of batteries and non-uniform temperature distribution, which further lead to reduction of cycle life and battery capacity over time. To solve this problem, this work uses experimental and numerical methods to conduct a comprehensive investigation on the clustering of battery cells with similar performance in order to produce a battery module with improved electrochemical performance. Experiments were first performed by dismantling battery modules for the measurement of performance parameters. The k-means clustering and support vector clustering (SVC) algorithms were then employed to produce battery modules composed of 12 cells each. Experimental verification of the results obtained from the clustering analysis was performed by measuring the temperature rise in the cells over a certain period, while air cooling was provided. It was found that the SVC-clustered battery module in Category 3 exhibited the best performance, with a maximum observed temperature of 32 °C. By contrast, the maximum observed temperatures of the other battery modules were higher, at 40 °C for Category 1 (manufacturer), 36 °C for Category 2 (manufacturer), and 35 °C for Category 4 (k-means-clustered battery module).

1. Introduction

Energy-storage systems such as battery modules for new energy vehicles (NEVs) are gaining extensive attention [1,2] as a means of replacing traditional gas (petrol/diesel)-operated vehicles and thereby promoting a cleaner environment. The performance parameters of lithium (Li)-ion battery modules include energy density, capacity, and specific power. To meet the power demand required for the transmission systems of NEVs, several small battery modules are used in series or parallel to form a large battery module (also known as a battery pack). A battery module consists of a number of cells connected in series and parallel. The range of an NEV depends on the performance of its battery module, and the performance of a battery module depends on the individual performance of each cell and on the configuration of the cells in series or parallel. The ideal performance of a battery module should follow

the criteria of uniformity and equalization; however, these criteria have not yet been satisfactorily met.

During the mass manufacturing of cells and the assembly of cells into modules, slight variations occur due to uncertainties in the operating manufacturing conditions [3]; these may include a performance difference of the electrode materials, a change of operating conditions, or geometrical variation caused by machining errors [4]. These uncertainties can cause defects in the battery modules such as surface scratches, exposed foils, and cracks. Manufacturing defects in battery modules lead to variations in performance among the cells used in series or parallel configuration, which in turn may lead to variations in the performance parameters (i.e., capacity and voltage) of each cell in a module. Over a period of time, this problem accumulates, resulting in uneven temperature distribution and incomplete charge/discharge of several cells in the module. These problems lead to less capacity being available [5–7].

Uniformity and equalization criteria—if adapted during the design and manufacturing of a battery module—can avoid the

* Corresponding author.
E-mail address: gaoliang@mail.hust.edu.cn (L. Gao).

problems of overheating, thermal runaway, and so forth, and thus increase the life of the battery module [8–12].

In order to solve these problems, some battery-sorting methods have been researched [13–15]. Gallardo-Lozano et al. [16] summarized the different active methods for a battery equalization system, and concluded that the switched capacitor and double-tiered switching capacitor methods are the best sorting methods. Kim et al. [17] proposed an approach based on a screening process (capacity screening and resistance screening) to improve the utility of a Li-ion series battery module. In subsequent research, they proposed a practical universal modeling of multi-cell battery strings arranged in series and parallel configurations [18]. Kim et al. [19] proposed a modularized two-stage charge equalizer with cell selection switches. The advantage of this sorting method is that it can be widely used for a large number of Li-ion cells in a hybrid electric vehicle (HEV). In addition, five sorting methods—namely, capacity and alternate current internal resistance, electrochemical impedance spectroscopy (EIS), voltage curve, dynamics parameters, and thermal behavior—are compared in Ref. [20]. It was found that low-frequency battery impedance is the most suitable method for sorting batteries by their dynamic characteristics.

Previous studies [21–36] have conducted the selection and classification of homogenous cells. Based on experimental verification, the sorted cells have a more consistent performance in terms of voltage, temperature, and capacity in comparison with unsorted cells. However, little research has focused on conducting experiments. Therefore, the present work combines experimental and numerical methods to conduct a comprehensive investigation on the clustering of battery cells with similar performance in order to design a battery module with higher electrochemical performance. Fig. 1 illustrates the procedures that were used to perform the clustering analysis and verify the performance of the designed modules. Charging–discharging tests were conducted on 48 Li-ion cells to measure their voltage, temperature, and capacity. The k-means clustering and support vector clustering (SVC) algorithms were used to group cells with similar performance in order to produce a battery module. A comparison analysis was performed on the performance of the battery modules produced in this research and the performance of those purchased from a manufacturer.

2. Experimental setup for data measurement

This section describes the charging–discharging tests that were conducted on 48 Li-ion cells for the measurement of data (voltage, temperature, and capacity). The 48 cells were obtained by dismantling the battery pack shown in Fig. 2(a).

The disassembly process of the battery modules was performed in four steps:

Step 1: Obtain information on the battery modules such as capacity, cell numbers, and connection modes between cells.

Step 2: Identify the output terminal of the battery module once the module is unpacked. This step should be done carefully to avoid any connection between the negative and positive poles of the battery module.

Step 3: Break the series connection first. In order to ensure safety, the battery module was split up into small parts by destroying the series and parallel connections.

Step 4: Split the small parts into cells.

After dismantling the battery module, charging–discharging tests were conducted by means of a battery-testing system (Fig. 2(b)). The battery-testing system mainly include the battery-testing device, a data-collecting system, Li-ion cells, etc. The battery-testing device was purchased from Newware Ltd. It has eight channels and can save data automatically. The steps for testing the charging–discharging process are summarized in Table 1. Step 1: The constant current discharge was set at 1.3 A. Step 2: This step began at the point when the voltage of the Li-ion battery was 2.75 V, and involved a resting time of 30 min. Step 3: A constant current and constant voltage charge were set with a cut-off voltage of 4.2 V. Step 4: This step again involved resting for 30 min. Step 5: The number of cycles was set as 20. Throughout the process, the voltage was not permitted to exceed the range of 2.65–4.3 V. Each cell was charged–discharged for at least 30 cycles. The data collected from the experiment are shown in Table 2, where
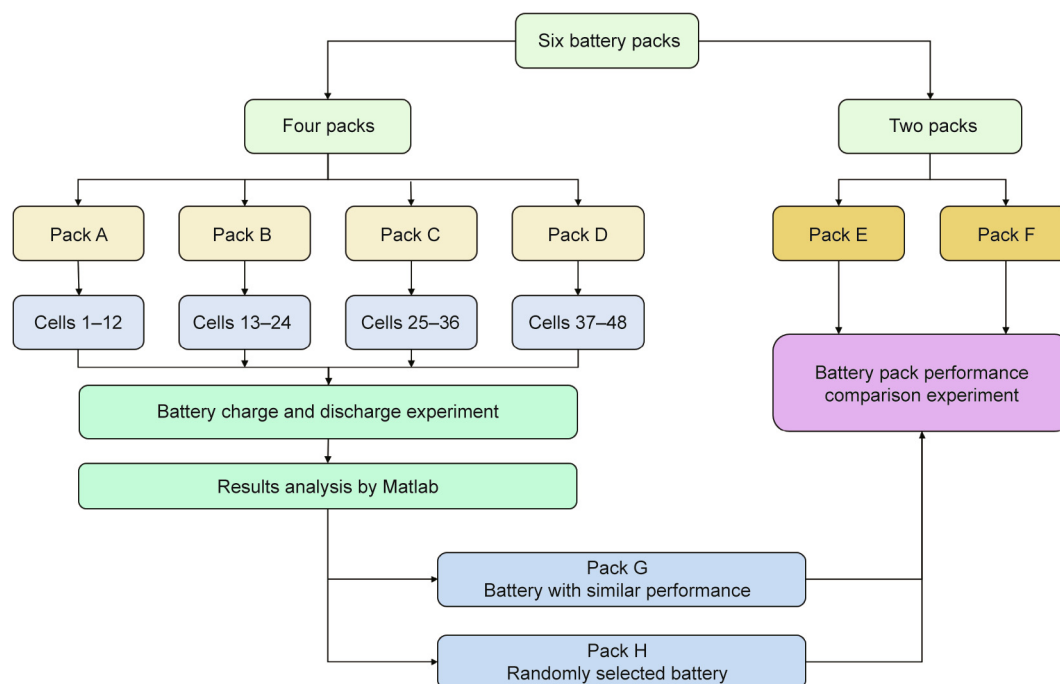

Fig. 1. A comprehensive procedure for the design and manufacture of a battery module.
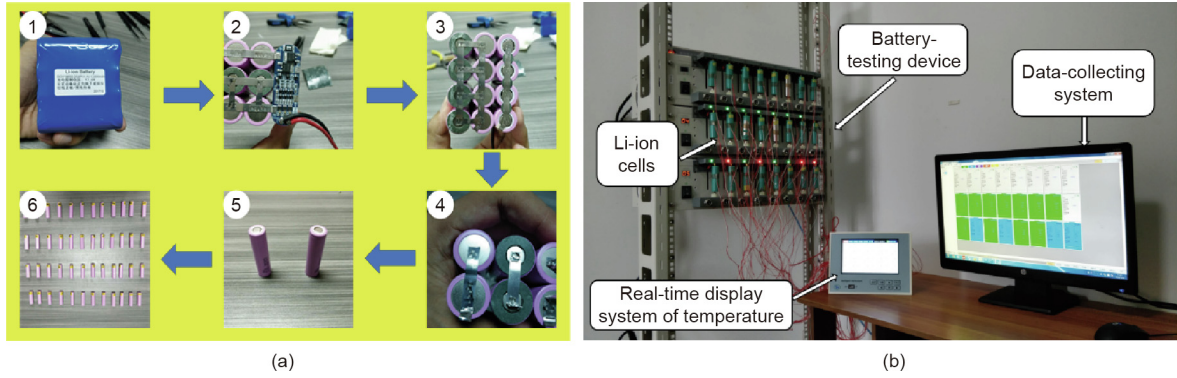
Fig. 2. (a) Dismantling and disassembly process for battery modules; (b) battery–testing system used for conducting charging–discharging tests.

Table 1
Steps for testing the 18650 Li-ion battery.

Step	State	Value	Cut-off voltage
1	Constant current discharge	1.3 A	2.75 V
2	Resting	30 min	
3	Constant current and constant voltage charge	1.3 A 4.2 V	4.2 V
4	Resting	30 min	
5	Cycle	20	

Maximum safety voltage: 4.3 V; minimum safety voltage: 2.65 V; start experiment steps: constant current discharge.

"zero" and "full" refer to fully discharged and fully charged states, respectively. The following section describes how clustering algorithms were used to analyze the collected experimental data.

3. Clustering algorithms

Supervised learning and unsupervised learning are two categories of machine learning methods. Supervised learning is generally used for classification, while unsupervised learning is employed for clustering. Clustering algorithms are a broad set of techniques for grouping data according to different rules; many excellent descriptions can be found in Refs. [37–39]. The purpose of clustering analysis is to group data into several classes according to certain rules. These classes are not given in advance, but are determined by the characteristics of the data. The data in the same class tend to resemble each other in a sense, whereas the data in different classes tend to be discrepant.

3.1. k-means clustering algorithm

MacQueen proposed the k-means clustering algorithm in 1967 [39]. As this algorithm is simple and easy to understand and has a relatively fast calculation speed, it is usually used as the preferred algorithm for the cluster analysis of large samples [40].

The main steps of the k-means clustering algorithm are as follows:

Step 1: k samples are randomly selected as the initial cluster centers.

Step 2: The distances between other data and each initial cluster center are calculated, and the data are divided into cluster domains in which the nearest cluster center is located.

Step 3: After all the data are sorted, the average of all the data of every cluster is recalculated, and the data where the average is located become a new cluster center.

Step 4: Multiple iterations are performed until the centers of two consecutive clusters are the same, indicating that the data are classified into k clusters.

The sum of square errors is a commonly used evaluation criterion that refers to the sum of the Euclidean distances from the data samples in one cluster to the cluster center m_l, which can be expressed as follows:

$$E(m_1, m_2, ..., m_l) = \sum_{i=1}^{k} \sum_{j \in c_l} \| \mathbf{x}_j - m_l \|^2 \tag{1}$$

where $\{\mathbf{x}_j\} \subseteq \gamma$ is a dataset, $\gamma \subseteq \Omega$ is the data domain, k is the number of clusters, and c_l is the cluster domain whose cluster center is m_l. The clustering center m_l can be calculated by the following:

$$m_l = \frac{1}{N_l} \sum_{j \in c_l} \mathbf{x}_j \tag{2}$$

where N_l is the number of data samples in clustering domain c_l.

The objective function $E(\cdot)$ in Eq. (1) represents the sum of the square errors between all the data in k clusters and their cluster center m_l. A smaller value of $E(\cdot)$ indicates better data concentration in the cluster—that is, a better clustering result.

Although the k-means clustering algorithm is practical and simple to implement, it has some limitations. First, determining a reasonable value of k is difficult. Second, the randomness of selecting initial clustering centers may result in instability of the clustering results. Third, this algorithm is sensitive to noise. A self-organized map based on a neural network can also be used for clustering. However, it is necessary to train the neural networks, which can make this process time-consuming. Therefore, the next section introduces a better and more efficient clustering algorithm.

3.2. The SVC algorithm

In general, a support vector machine (SVM) is adopted for classification (supervised learning). SVC is a slightly different algorithm from an SVM. In fact, SVC is an unsupervised learning clustering algorithm.

The main idea of SVC is to map data space to a high-dimensional feature space using a Gaussian kernel function. Next, a sphere with a minimum radius is obtained and the sphere contains most of the mapped data [41,42]. After being mapped back to the data space, the sphere can be separated into several parts, each containing a single cluster point set.

In this paper, a robust and efficient cluster marking method is adopted, which is based on the training kernel radius function. This method has two stages. The first stage involves dividing the dataset into several mutually exclusive groups, each of which is a cluster. The second stage involves marking all data samples.

The description of the dataset support vector is the foundation of the SVC algorithm. The data samples are mapped to a high-dimensional feature space through nonlinear changes, and the

Table 2
Data obtained from charging–discharging tests on cells.

Cell number	Discharged state			Charged state		
	Zero voltage (V)	Zero temperature (°C)	Zero capacity (A·h)	Full voltage (V)	Full temperature (°C)	Full capacity (A·h)
1	3.3981	25.6	2.6783	4.1895	26.0	2.6847
2	3.3751	26.8	2.7192	4.1911	26.9	2.7258
3	3.4065	26.6	2.6669	4.1887	26.9	2.6683
4	3.3557	26.5	2.6959	4.1922	26.5	2.7056
5	3.4055	26.7	2.4773	4.1905	26.8	2.4843
6	3.3600	26.1	2.6488	4.1882	26.2	2.6538
7	3.3649	25.8	2.6845	4.1900	26.1	2.6858
8	3.3981	25.6	2.6783	4.1895	26.0	2.6847
9	–	–	–	–	–	–
10	3.4128	28.0	2.6941	4.1946	26.6	2.6934
11	3.3774	27.9	2.6698	4.1962	27.3	2.6533
12	3.3769	28.0	2.7042	4.1946	27.0	2.7080
13	3.3884	27.9	2.6861	4.1941	26.7	2.6881
14	3.3464	26.8	2.6829	4.1946	26.3	2.6349
15	3.3908	27.1	2.6764	4.1949	26.7	2.6571
16	3.4147	26.9	2.6617	4.1953	26.4	2.6646
17	3.4103	25.3	2.5432	4.1954	24.8	2.5468
18	3.4063	24.2	2.6620	4.1947	23.6	2.6594
19	3.4089	23.7	2.6707	4.1938	24.0	2.6737
20	3.3982	25.1	2.6708	4.1946	23.0	2.6717
21	3.4182	24.2	2.5175	4.1941	24.1	2.5170
22	3.3995	23.8	2.6642	4.1944	22.4	2.6634
23	3.3939	23.2	2.6728	4.1951	22.7	2.6724
24	3.4041	22.9	2.6348	4.1936	22.9	2.6323
25	3.3967	28.3	2.6452	4.1966	28.6	2.6455
26	3.4026	29.3	2.6413	4.1965	29.0	2.6434
27	3.4011	23.8	2.6851	4.1962	24.3	2.6877
28	3.3962	28.3	2.6560	4.1962	29.6	2.6634
29	3.4154	23.8	2.5792	4.1950	23.7	2.5837
30	3.2876	28.8	2.6331	4.1941	30.5	2.6364
31	3.4122	29.9	2.5995	4.1944	30.1	2.5987
32	3.4104	30.1	2.6747	4.1947	30.1	2.6790
33	3.3937	25.0	2.6566	4.1945	24.8	2.6534
34	3.3790	25.1	2.6788	4.1948	24.2	2.6756
35	3.3902	24.8	2.6020	4.1951	24.4	2.6022
36	–	–	–	–	–	–
37	3.4002	23.8	2.6394	4.1943	23.8	2.6386
38	3.3851	23.8	2.6446	4.1956	23.5	2.6434
39	3.4251	23.8	2.6228	4.1927	23.7	2.6192
40	3.4100	24.7	2.5946	4.1953	24.7	2.5933
41	3.3533	25.3	2.6293	4.1962	25.1	2.6310
42	3.3960	25.3	2.6796	4.1958	24.6	2.6776
43	3.3964	25.4	2.6917	4.1964	25.2	2.6955
44	3.3601	25.2	2.6931	4.1952	24.4	2.6953
45	3.4027	23.9	2.6643	4.1941	23.5	2.6663
46	3.3747	23.8	2.6763	4.1952	23.7	2.6750
47	3.3881	24.2	2.6236	4.1952	23.6	2.6268
48	–	–	–	–	–	–

minimum radius of a sphere containing all the mapped data samples is identified. The above steps are equivalent to the following optimization problem:

$$\max W = \sum_j \Phi(\mathbf{x}_j)^2 \beta_j - \sum_{i,j} \beta_i \beta_j \Phi(\mathbf{x}_i) \cdot \Phi(\mathbf{x}_j)$$
$$\text{s.t. } 0 \le \beta_j \le C, \sum_j \beta_j = 1, j = 1, ..., N \tag{3}$$

where $\Phi(\cdot)$ represents the nonlinear mapping, β_j is the Lagrange multiplier, and C is a regularization constant. Only the samples that satisfy the constraints $0 \le \beta_j \le C$ lie on the boundary of the sphere. When $\beta_j = C$, the samples are located outside the boundary. The Gaussian kernel function is used to calculate the dot product $\Phi(\mathbf{X}_i) \cdot \Phi(\mathbf{X}_j)$:

$$K(\mathbf{x}_i, \mathbf{x}_j) = e^{-q\|\mathbf{x}_i - \mathbf{x}_j\|^2} \tag{4}$$

where q is the width parameter and W can be re-expressed as follows:

$$W = \sum_j K(\mathbf{x}_j, \mathbf{x}_j)\beta_j - \sum_{i,j} \beta_i \beta_j K(\mathbf{x}_i, \mathbf{x}_j) \tag{5}$$

At each point of $\mathbf{x}_i$, W is defined as the Wolfe dual form of the distance from the center of the sphere in the feature space.

$$f(\mathbf{x}) = R^2(\mathbf{x}) = \| \Phi(\mathbf{x}) - a \|^2 \tag{6}$$

where $R(\cdot)$ is the distance from each $\mathbf{x}_i$ to the center of the sphere and a is the center of the sphere. Considering the kernel definition, the following equation can be obtained:

$$f(\mathbf{x}) = R^2(\mathbf{x}) = K(\mathbf{x}, \mathbf{x}) - 2\sum_j K(\mathbf{x}_j, \mathbf{x})\beta_j + \sum_{i,j} \beta_i \beta_j K(\mathbf{x}_i, \mathbf{x}_j) \tag{7}$$

A notable feature of the trained kernel radius function is that this cluster boundary can be constructed from a set of outlines to contain samples in data space: $\left\{ \mathbf{x} : f(\mathbf{x}) = \hat{R}^2 \right\}$, $\hat{R} = R(X_i)$ for a support vector $\mathbf{x}_i$. $f(\cdot)$ is separated into several disjointed sets:

$$L_f\left(\hat{R}^2\right) = \left\{\mathbf{x} : f(\mathbf{x}) = \hat{R}^2\right\} = C_1 \cup \ldots \cup C_n \tag{8}$$

where C_i ($i = 1,\ldots, n$) is the connection set corresponding to different clusters.

Although it may be difficult to determine the appropriate kernel parameters in the selection of the model, SVC has some obvious advantages over other clustering algorithms: ① It can generate arbitrary cluster boundary shapes; ② it has flexible boundary changes to handle outliers; and ③ it avoids explicit calculations and is therefore effective for large datasets.

3.3. Clustering results

Supervised learning methods require training sets and test sets. This method identifies the rules in the training set and then uses these rules for the test set. In contrast, unsupervised learning has no training set or test set; rather, it looks for rules only in a set of data. In this research, the six kinds of parameters of charged and discharged state in Table 2 were used as the input vectors to conduct the clustering analysis. The output is the clustering results, which were verified by performing experimental verification.

This section mainly focuses on the clustering analysis of the data in Table 2. In this study, we chose voltage, temperature, and capacity as the inputs. Of course, researchers can also choose other parameters, so this choice of inputs is just one option rather than a standard. In this paper, the k-means clustering and the SVC algorithms are considered. In the SVC approach, the kernel argument q and the regularization constant C are set as 0.2 and 1.2, respectively. In the k-means clustering approach, the number of clusters is set as 4. The results of the clustering analysis are shown in Table 3, where the column labeled "un-clustering" represents the comparison group that is produced by randomly selected cells out of all the cells.

Based on the clustering analysis results, the changes in voltage, temperature, and capacity in the charge and discharge of the new battery module were calculated. The mean difference and standard difference were calculated by the following:

$$m_{\mathrm{v}} = \frac{1}{N} \sum_{i=1}^{N} \left(F_{\mathrm{v}_i} - Z_{\mathrm{v}_i}\right) \tag{9}$$

$$s_{\mathrm{v}} = \sqrt{\frac{1}{N} \sum_{i=1}^{N} \left(F_{\mathrm{v}_i} - Z_{\mathrm{v}_i} - m_{\mathrm{v}}\right)^2} \tag{10}$$

where m_{v} denotes the mean difference of the voltage; F_{v} and Z_{v} denote the full voltage and zero voltage, respectively; N is the number of cells; and s_{v} denotes the standard difference of the voltage.

The results of the mean difference and standard difference are given in Tables 4 and 5, respectively. As can be seen from Table 4, the mean differences of the voltage, temperature, and capacity in the sorted battery module are obviously smaller than those in the unsorted battery module, indicating that the sorted cells share a similar performance. The results in Tables 4 and 5 are also represented in Figs. 3 and 4, respectively. From Fig. 3, it can be seen that the SVC algorithm performed better than the k-means clustering algorithm in the clustering analysis, especially regarding temperature difference.

4. Experimental verification

In order to verify the results of the clustering, experimental verification was performed. As temperature is the most important parameter affecting the capacity and life of a battery module, an analysis was performed on the temperatures (performance parameter) of the battery modules produced from the four different

Table 3
Clustering analysis results.

Clustering method	Cell number
Un-clustering	4, 7, 21, 22, 23, 24, 26, 27, 29, 30, 42, 44
k-means clustering	18, 19, 22, 23, 27, 29, 37, 38, 39, 45, 46, 47
SVC	17, 18, 21, 23, 24, 27, 29, 33, 35, 39, 40, 41

Table 4
Mean difference of battery module.

Clustering method	Voltage (V)	Temperature (°C)	Capacity (A·h)
Un-clustering	0.8111	0.5541	0.0026
k-means clustering	0.7946	0.4183	0.0022
SVC	0.7930	0.2762	0.0022

Table 5
Standard difference of battery module.

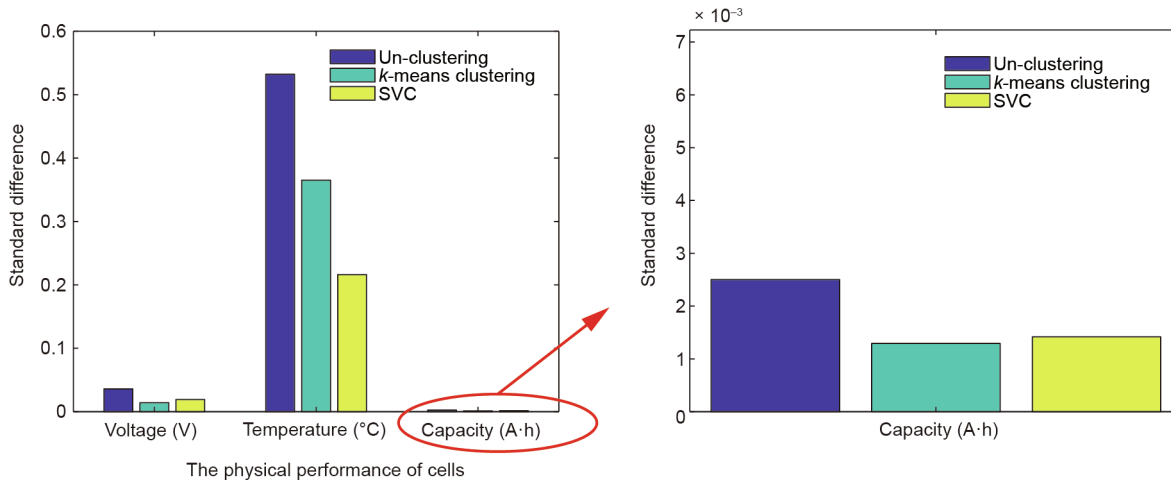| Clustering method	Voltage (V)	Temperature (°C)	Capacity (A·h)
Un-clustering	0.0360	0.5322	0.0025
k-means clustering	0.0142	0.3652	0.0013
SVC	0.0191	0.2162	0.0014
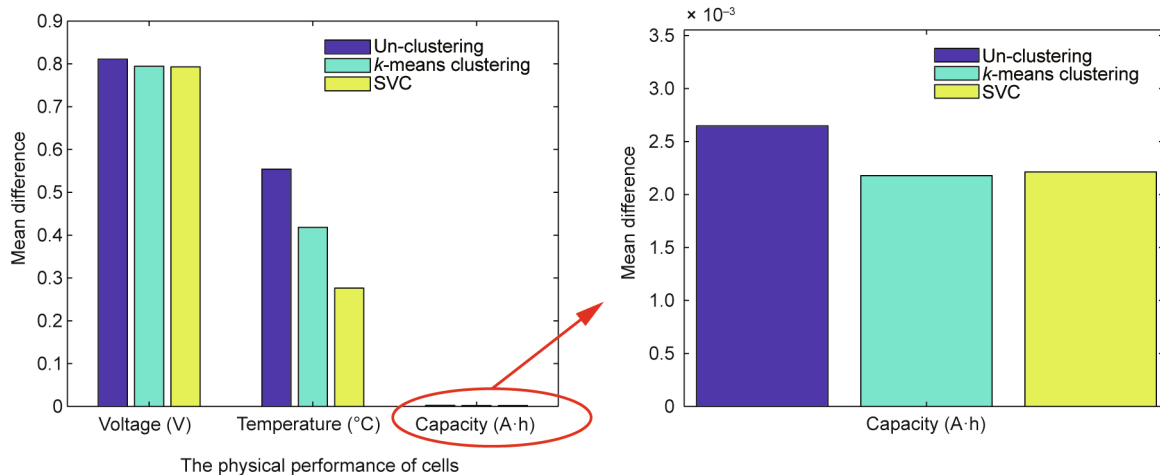
Fig. 3. Mean difference of battery module.

Fig. 4. Standard difference of battery module.

categories (i.e., two modules purchased from the manufacturer with the same specifications, one SVC-clustered battery module, and one k-means-clustered battery module produced from the grouping of cells). The experimental setup is shown in Fig. 5. Air cooling was supplied from the bottom for the modules of each category. The temperature was observed every 5 min over the cycle as the module was charged–discharged at the same rate. Fig. 6 clearly shows that the battery modules corresponding to Category 3 (the SVC-clustered battery module) presented the best performance,

with a maximum observed temperature of 32 °C. By contrast, the maximum observed temperatures of the other battery modules were higher, at 40 °C for Category 1 (manufacturer), 36 °C for Category 2 (manufacturer) and 35 °C for Category 4 (k-means-clustered battery module). As the SVC-clustered battery module underwent the least heating, it is expected to have a longer life-cycle than the modules in the other categories. A plausible reason for this result is that the selection of cells with similar performance that was made when producing the module resulted in an
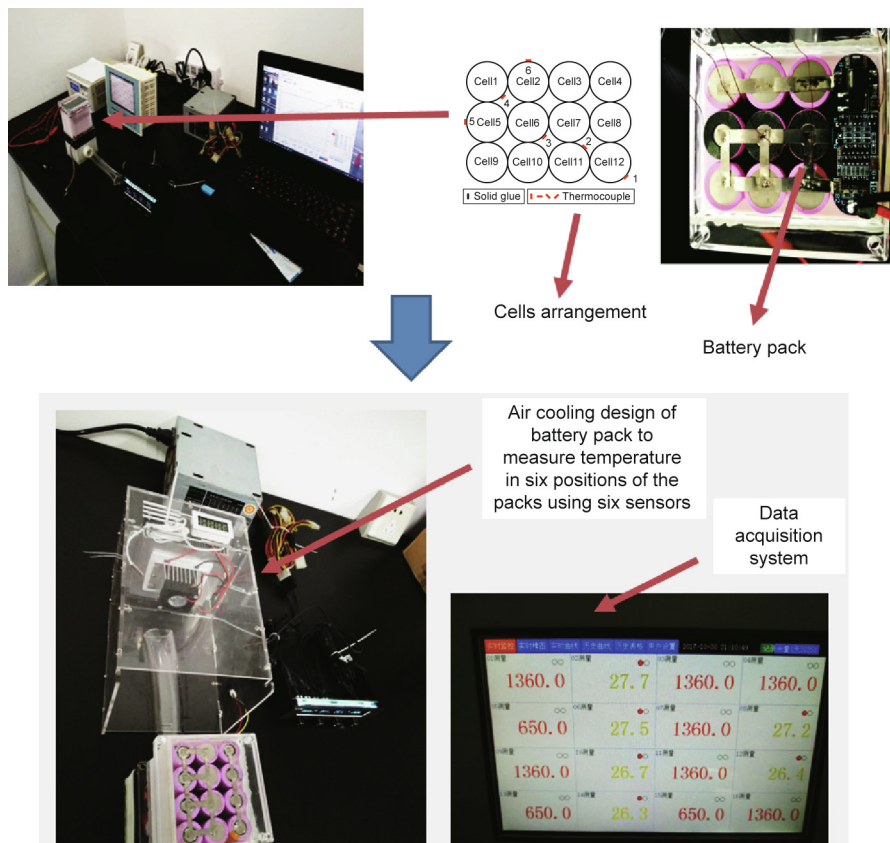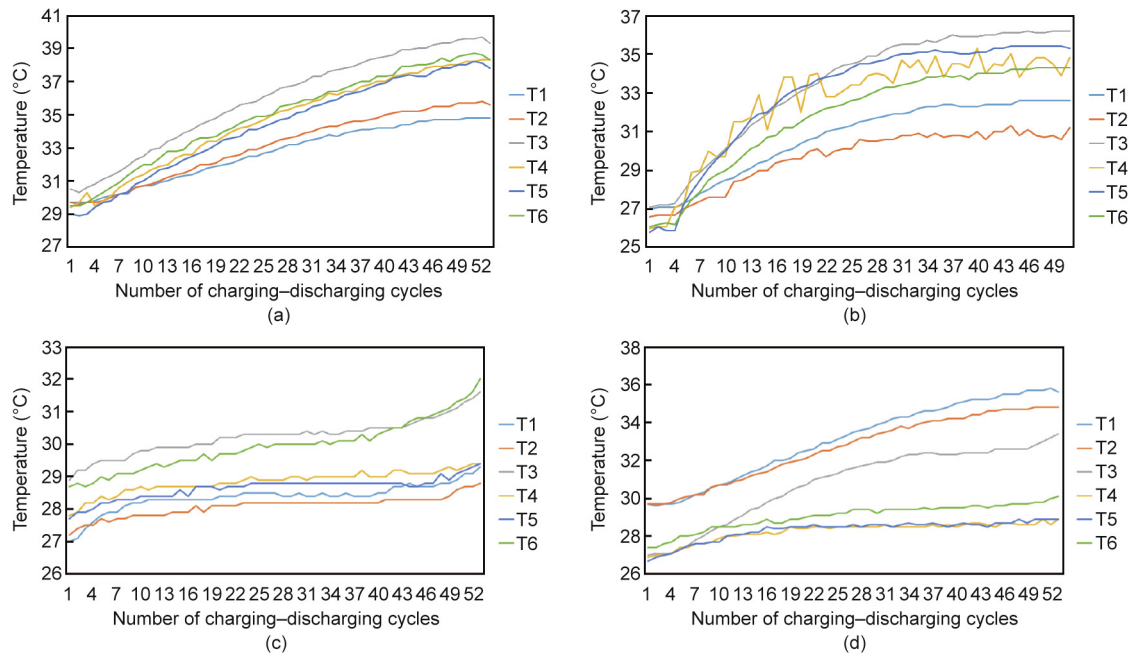

Fig. 5. Experimental setup for the verification of the produced battery modules.

Fig. 6. Temperature variation of the battery modules at six different positions in a charging–discharging cycle from four categories: (a) Category 1 (manufacturer); (b) Category 2 (manufacturer); (c) Category 3 (SVC-clustered battery module); (d) Category 4 (k-means-clustered battery module).

equalized temperature distribution within the module, which consequently lowered the rise in temperature in comparison with the modules in the other categories.

5. Conclusions

To achieve uniformity and equalization of the Li-ion cells used in a battery module for NEVs, we combined experimental and numerical methods to conduct a comprehensive investigation on the clustering of battery cells with similar performance in order to design a battery module with better electrochemical performance. Charging–discharging tests were performed on 48 cells. Clustering algorithms were then employed to conduct a clustering analysis on the two kinds of battery modules (a SVC-clustered battery module and a k-means-clustered battery module). The performances of the battery modules created using clustering algorithms were compared with the performances of the two modules purchased from a manufacturer. The SVC-clustered battery module exhibited the best performance, with a maximum observed temperature of 32 °C. By contrast, the maximum observed temperatures of the other battery modules were higher, at 40 °C for Category 1 (manufacturer), 36 °C for Category 2 (manufacturer), and 35 °C for Category 4 (k-means-clustered battery module). A plausible reason for this finding is that the selection of cells with similar performance during the production of the module resulted in an equalized temperature distribution within the module, which consequently lowered the rise in temperature in comparison with the modules in the other categories.

The k-means clustering algorithm performance may vary depending on the data used. However, for the SVC algorithm, if the data are given, the clustering results are only affected by the SVC parameter settings. Furthermore, since SVC avoids explicit calculations in the high-dimensional feature space, it is effective for large datasets. It can easily be applied in industrial contexts in which the electric vehicles comprise hundreds of packs.

In order to minimize battery manufacturing defects, the processing technology and assembly level can be improved; alternatively, the ability to detect defects can be improved. However, manufacturing defects do exist. Although the proposed approach may appear to be overly lengthy for incorporation before the design stage, it is worth noting that an alternative application of the proposed method could be for battery recycling. Since batteries contain chemical substances and heavy metals, their disposal can cause environmental pollution and a waste of resources. However, old batteries still have various levels of capacity that can be used in other areas. Future work can focus on conducting large-scale testing on cells in order to design a larger battery module, as well as on performing experimental verification on the performance of probabilistic methods [43,44], extreme machine learning methods [45,46], and artificial-intelligence-based methods [47–50].

Compliance with ethics guidelines

Wei Li, Siqi Chen, Xiongbin Peng, Mi Xiao, Liang Gao, Akhil Garg, and Nengsheng Bao declare that they have no conflict of interest or financial conflicts to disclose.

References

[1] Choi JW, Aurbach D. Promise and reality of post-lithium-ion batteries with high energy densities. Nat Rev Mater 2016;1(4):16013.
[2] Wen F, Lin C, Jiang JC, Wang ZG. A new evaluation method to the consistency of lithium-ion batteries in electric vehicles. In: Proceedings of 2012 Asia-Pacific

Power and Energy Engineering Conference; 2012 Mar 27–29; Shanghai, China; 2012.

[3] Mohanty D, Hockaday E, Li J, Hensley DK, Daniel C, Wood III DL. Effect of electrode manufacturing defects on electrochemical performance of lithium-ion batteries: cognizance of the battery failure sources. J Power Sources 2016;312:70–9.

[4] Hong L, Li LS, Chen-Wiegart YK, Wang JJ, Xiang K, Gan LY, et al. Two-dimensional lithium diffusion behavior and probable hybrid phase transformation kinetics in olivine lithium iron phosphate. Nat Commun 2017;8(1):1194.

[5] Fang KZ, Chen S, Mu DB, Wu BR, Wu F. Investigation of nickel-metal hydride battery sorting based on charging thermal behavior. J Power Sources 2013;224:120–4.

[6] Shi W, Hu XS, Jin C, Jiang JC, Zhang YR, Yip T. Effects of imbalanced currents on large-format LiFePO$_4$/graphite batteries systems connected in parallel. J Power Sources 2016;313:198–204.

[7] Yang NX, Zhang XW, Shang BB, Li GJ. Unbalanced discharging and aging due to temperature differences among the cells in a lithium-ion battery pack with parallel combination. J Power Sources 2016;306:733–41.

[8] Brand MJ, Hofmann MH, Steinhardt M, Schuster SF, Jossen A. Current distribution within parallel-connected battery cells. J Power Sources 2016;334:202–12.

[9] Dubarry M, Devie A, Liaw BY. Cell-balancing currents in parallel strings of a battery system. J Power Sources 2016;321:36–46.

[10] Wei X, Zhu B. The research of vehicle power Li-ion battery pack balancing method. In: Proceedings of the 9th International Conference on Electronic Measurement & Instruments; 2009 Aug 16–19; Beijing, China; 2009.

[11] Park SH, Park KB, Kim HS, Moon GW, Youn MJ. Single-magnetic cell-to-cell charge equalization converter with reduced number of transformer windings. IEEE Trans Power Electr 2012;27(6):2900–11.

[12] Sun FC, Xiong R. A novel dual-scale cell state-of-charge estimation approach for series-connected battery pack used in electric vehicles. J Power Sources 2015;274:582–94.

[13] Moore SW, Schneider PJ. A review of cell equalization methods for lithium ion and lithium polymer battery systems. SAE Technical Paper. Warrendale: Society of Automotive Engineers, Inc.; 2001. Report No.: 2001-01-0959.

[14] Pei L, Zhu CB, Wang TS, Lu RG, Chan CC. Online peak power prediction based on a parameter and state estimator for lithium-ion batteries in electric vehicles. Energy 2014;66:766–78.

[15] An FQ, Huang J, Wang CY, Li Z, Zhang JB, Wang S, et al. Cell sorting for parallel lithium-ion battery systems: evaluation based on an electric circuit model. J Energy Storage 2016;6:195–203.

[16] Gallardo-Lozano J, Romero-Cadaval E, Milanes-Montero MI, Guerrero-Martinez MA. Battery equalization active methods. J Power Sources 2014;246:934–49.

[17] Kim J, Shin J, Chun C, Cho BH. Stable configuration of a Li-ion series battery pack based on a screening process for improved voltage/SOC balancing. IEEE Trans Power Electr 2012;27(1):411–24.

[18] Kim J, Cho BH. Screening process-based modeling of the multi-cell battery string in series and parallel connections for high accuracy state-of-charge estimation. Energy 2013;57:581–99.

[19] Kim CH, Kim MY, Park HS, Moon GW. A modularized two-stage charge equalizer with cell selection switches for series-connected lithium-ion battery string in an HEV. IEEE Trans Power Electr 2012;27(8):3764–74.

[20] Li XY, Wang TS, Pei L, Zhu CB, Xu BL. A comparative study of sorting methods for lithium-ion batteries. In: Proceedings of 2014 IEEE Conference and Expo Transportation Electrification Asia-Pacific; 2014 Aug 31–Sep 3; Beijing, China; 2014.

[21] Wang Q, Cheng XZ, Wang J. A new algorithm for a fast testing and sorting system applied to battery clustering. In: Proceedings of the 6th International Conference on Clean Electrical Power; 2017 Jun 27–29; Santa Margherita Ligure, Italy. Piscataway: IEEE; 2017. p. 397–402.

[22] Enami N, Moghadam RA. Energy based clustering self organizing map protocol for extending wireless sensor networks lifetime and coverage. Can J Multimed Wirel Netw 2010;1(4):42–54.

[23] Raspa P, Frinconi L, Mancini A, Cavalletti M, Longhi S, Fulimeni L, et al. Selection of lithium cells for EV battery pack using self-organizing maps. Automot Saf Energy Technol 2011;2:32–9.

[24] Piao CH, Wang ZG, Cao J, Zhang W, Lu S. Lithium-ion battery cell-balancing algorithm for battery management system based on real-time outlier detection. Math Probl Eng 2015;2015:168529.

[25] Ma Y, Duan P, Sun YS, Chen H. Equalization of lithium-ion battery pack based on fuzzy logic control in electric vehicle. IEEE Trans Ind Electron 2018;65(8):6762–71.

[26] He F, Shen WX, Song Q, Kapoor A, Honnery D, Dayawansa D. Clustering LiFePO$_4$ cells for battery pack based on neural network in EVs. In: Proceedings of 2014 IEEE Conference and Expo Transportation Electrification Asia-Pacific; 2014 Aug 31–Sep 3; Beijing, China; 2014.

[27] Li XY, Song K, Wei G, Lu RG, Zhu CB. A novel grouping method for lithium iron phosphate batteries based on a fractional joint Kalman filter and a new modified k-means clustering algorithm. Energies 2015;8(8):7703–28.

[28] Yang YX, Gao MY, He ZW, Wang CS. A robust battery grouping method based on a characteristic distribution model. Energies 2017;10(7):1035.

[29] Lee KM, Chung YC, Sung CH, Kang B. Active cell balancing of Li-ion batteries using LC series resonant circuit. IEEE Trans Ind Electron 2015;62(9):5491–501.

[30] Shang YL, Zhang CH, Cui NX, Guerrero JM. A cell-to-cell battery equalizer with zero-current switching and zero-voltage gap based on quasi-resonant LC converter and boost converter. IEEE Trans Power Electr 2015;30(7):3731–47.

[31] Lee KM, Lee SW, Choi YG, Kang B. Active balancing of Li-ion battery cells using transformer as energy carrier. IEEE Trans Ind Electron 2017;64(2):1251–7.

[32] Einhorn M, Roessler W, Fleig J. Improved performance of serially connected Li-ion batteries with active cell balancing in electric vehicles. IEEE Trans Veh Technol 2011;60(6):2448–57.

[33] Zheng YJ, Lu LG, Han XB, Li JQ, Ouyang MG. LiFePO$_4$ battery pack capacity estimation for electric vehicles based on charging cell voltage curve transformation. J Power Sources 2013;226:33–41.

[34] Zhong L, Zhang CB, He Y, Chen ZH. A method for the estimation of the battery pack state of charge based on in-pack cells uniformity analysis. Appl Energy 2014;113:558–64.

[35] Zheng YJ, Ouyang MG, Lu LG, Li JQ, Han XB. Xu LF. On-line equalization for lithium-ion battery packs based on charging cell voltages: part 1. Equalization based on remaining charging capacity estimation. J Power Sources 2014;247:676–86.

[36] Samadi MF, Saif M. Nonlinear model predictive control for cell balancing in Li-ion battery packs. In: Proceedings of 2014 American Control Conference; 2014 Jun 4-6; Portland, OR, USA. Piscataway: IEEE; 2014. p. 2924–9.

[37] Xu R, Wunsch D Jr. Survey of clustering algorithms. IEEE Trans Neural Netw 2005;16(3):645–78.

[38] Tzortzis G, Likas A. The MinMax k-means clustering algorithm. Pattern Recognit 2014;47(7):2505–16.

[39] MacQueen J. Some methods for classification and analysis of multivariate observations. In: Proceedings of the Fifth Berkeley Symposium on Mathematical Statistics and Probability; 1965 Jun 21–Jul 18, 1965 Dec 27–1966 Jan 7; Berkeley, CA, USA. Berkeley: University of California Press; 1967. p. 281–97.

[40] Hung CH, Chiou HM, Yang WN. Candidate groups search for k-harmonic means data clustering. Appl Math Model 2013;37(24):10123–8.

[41] Ben-Hur A, Horn D, Siegelmann HT, Vapnik V. Support vector clustering. J Mach Learn Res 2001;2(12):125–37.

[42] Jun S, Park SS, Jang DS. Document clustering method using dimension reduction and support vector clustering to overcome sparseness. Expert Syst Appl 2014;41(7):3204–12.

[43] Garg A, Hazra B, Zhu H, Wen YP. A simplified probabilistic analysis of water content and wilting in soil vegetated with non-crop species. Catena 2019;175:123–31.

[44] Garg A, Bordoloi S, Mondal S, Ni JJ, Sreedeep S. Investigation of mechanical factor of soil reinforced with four types of fibers: an integrated experimental and extreme learning machine approach. J Nat Fibers 2018;2018:1–15.

[45] Garg A, Shankhwar K, Jiang D, Vijayaraghavan V, Panda BN, Panda SS. An evolutionary framework in modelling of multi-output characteristics of the bone drilling process. Neural Comput Appl 2018;29(11):1233–41.

[46] Garg A, Peng XB, Le MLP, Pareek K, Chin CMM. Design and analysis of capacity models for lithium-ion battery. Measurement 2018;120:114–20.

[47] Zhou WH, Tan F, Yuen KV. Model updating and uncertainty analysis for creep behavior of soft soil. Comput Geotech 2018;100:135–43.

[48] Tan F, Zhou WH, Yuen KV. Effect of loading duration on uncertainty in creep analysis of clay. Int J Numer Anal Methods Geomech 2018;42(11):1235–54.

[49] Panda B, Leite M, Biswal BB, Niu XD, Garg A. Experimental and numerical modelling of mechanical properties of 3D printed honeycomb structures. Measurement 2018;116:495–506.

[50] Panda BN, Garg A, Shankhwar K. Empirical investigation of environmental characteristic of 3-D additive manufacturing process based on slice thickness and part orientation. Measurement 2016;86:293–300.